

A Multiplexed Sonomyography System for Proprioceptive Proportional Control of Biomechatronic Interfaces

Anne Tryphosa Kamatham*, Azadeh Shariati ‡, Helge A. Wurdemann‡, and Biswarup Mukherjee*†

*Centre for Biomedical Engineering, Indian Institute of Technology Delhi, India.

†Department of Biomedical Engineering, All India Institute of Medical Sciences, New Delhi, India.

‡Department of Mechanical Engineering, University College London, UK.

bmukherjee@cbme.iitd.ac.in

Abstract—Sonomyography is an ultrasound-imaging-based technique that measures muscle activity. Real-time imaging of deep-seated muscle activity enables robust and intuitive biomechatronic control. However, the form factor of clinical ultrasound systems limits the practical utility of sonomyography. Therefore, recent investigations aim towards developing wearable ultrasound systems to utilize sonomyography for biomechatronic interfacing. In this paper, a wearable, multiplexed sonomyography transducer array for real-time sensing muscle activity has been presented. The forearm-muscle activity was quantified using a computationally inexpensive, correlation-based metric to generate a sonomyography signal. The sonomyography signal was then used to perform a human-computer interaction-based target achievement task involving one degree of freedom control in real-time. Results show that participants achieved the targets with an average success rate of $> 96\%$ for a target width of 10% , with minimal training. The results demonstrate the potential of a multiplexed sonomyography system for intuitive control of biomechatronic interfaces.

Index Terms—Sonomyography, Muscle activity sensing, Human-machine interfaces

I. INTRODUCTION

Dexterous and intuitive control of upper extremity prostheses requires modalities that could robustly sense the volitional movements from the residual muscles. Myoelectric prostheses controlled by surface electromyography (EMG) signals provide control over limited degrees of freedom with conventional two-site measurement [1]. Therefore, multi-channel and high-density electromyography (HD-EMG) measurements are employed for achieving sequential, simultaneous, proportional control [2] over multiple degrees of freedom, and gesture recognition using pattern recognition and machine learning techniques [3]. The pattern recognition method assumes the repeatability of patterns of muscle movements which could be affected by electrode shifts, and limb positions [4], thereby being ineffective in real-time control [5]. However, these

This work is supported in part by a Core Research Grant (CRG/2021/004967) from the Science and Engineering Research Board, Department of Science and Technology, Government of India (PI: Biswarup Mukherjee) and by a Multi-Institutional Faculty Interdisciplinary Research Program (MI02264G) under the UCL-IIT Delhi Strategic Partnership Fund (PIs: Biswarup Mukherjee, Helge A. Wurdemann).

systems still suffer from inherent limitations such as muscle cross-talk, poor signal-to-noise ratio, and signal instabilities. Additionally, EMG is incapable of measuring the activity of the deep muscles and individual muscle groups lacking spatial specificity. Therefore, there is a need for a wearable system for intuitive control of biomechatronic interfaces such as prostheses and assistive devices. Sonomyography is a non-invasive technique that uses ultrasound to measure muscle activity. Brightness-mode (B-mode) ultrasound images generated by clinical ultrasound systems allow visualization of the activity of the deep and superficial muscle groups, thereby providing excellent spatial specificity. The mechanical deformation of the muscles caused due to neural activation is an intuitive measure when quantified, as it indicates the presence of volitional movement. B-mode ultrasound images allow quantification of muscle deformation in real-time by tracking muscle structures such as cross-sectional area [6], muscle thickness [7], etc. Prior studies demonstrated gesture, and motion classification [8], finger forces [9], joint angle [10] estimation using B-mode systems corroborating the potential of ultrasound to achieve biomechatronic control [11], [12].

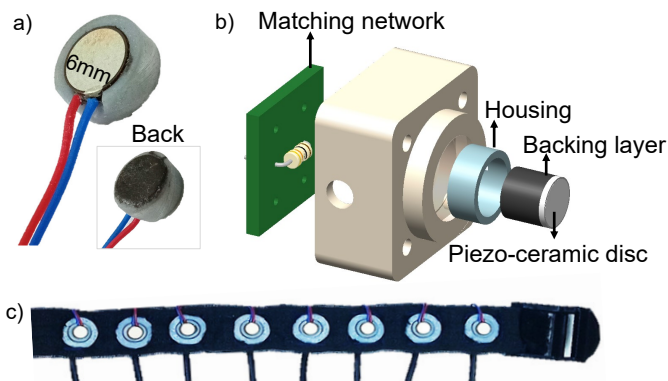


Fig. 1. a) Fabricated ultrasound transducer with backing layer b) CAD model showing the arrangement of the individual components of a single transducer c) Custom-developed 8-channel wearable sonomyography transducer array

Further, it has been shown that sonomyography-based proportional control techniques may tap into the proprioceptive feedback, thus enhancing the intuitiveness of control. To utilize sonomyography for biomechatronic control, the form factor of the clinical systems has to be significantly reduced. This can be achieved by using amplitude mode (A-mode) ultrasound signals which eliminates the need for the circuitry required to form the B-mode images. Recently, studies reported sparse B-mode images could achieve classification and force estimation accuracies [13], [14] comparable to those achieved using B-mode images. Recently, materials such as piezo-ceramic discs and flexible Polyvinylidene Fluoride (PVDF) are being explored to reduce the form factor of A-mode sonomyography transducers [15], [16]. A-mode signals measured from these transducers were mainly used to demonstrate real-time gesture recognition. Yang et al. developed a wearable ultrasound system [17] to demonstrate simultaneous proportional control of hand and wrist motions offline [18] and online [19].

In this paper, real-time measurement of muscle activity using a wearable multiplexed sonomyography system has been presented. The wearable sonomyography system consists of custom-developed single-element ultrasound transducers with a form factor suitable for integration with biomechatronic systems. The muscle activity was quantified using Pearson's correlation metrics to generate the sonomyography signal. This technique utilizes an unsupervised, model-free approach, thus obviating the need for model training. The sonomyography signal was used to perform a target achievement task in real-time involving proportional control over one degree of freedom by opening and closing the hand. The following sections detail the fabrication of a wearable sonomyography system and experiment design to demonstrate real-time control of target achievement task.

II. METHODS

A. Wearable sonomyography system

The wearable sonomyography system consists of the custom-developed sonomyography transducer array and the commercial ultrasound pulser-receiver. The wearable 8-channel sonomyography transducer array has been developed for sensing muscle activity. The single-element ultrasound transducers of the array were fabricated using piezo-ceramic discs made of Lead Zirconate Titanate (PZT) having a resonant frequency of 3 MHz (SMD063T07R111, Steiner & Martins Inc, USA). The backing layer was prepared by mixing 2 g of tungsten metal powder (325 Mesh, Central Drug House (P) Ltd., India) and 0.5 g of resin-hardener mixture (4:1 weight ratio, Araldite-Fevitite, Pidilite Industries, India) and was allowed to bind to the PZT. The backing layer was 3.5 mm thick. A purely inductive matching network was connected in parallel to the PZT to provide electrical matching. A 5 μ H inductor was used to match the resonant frequency of the PZT which has a static capacitance of 511 pF. The fabricated ultrasound transducer with a backing layer and matching network is shown in Fig. 1 a). The transducers were then

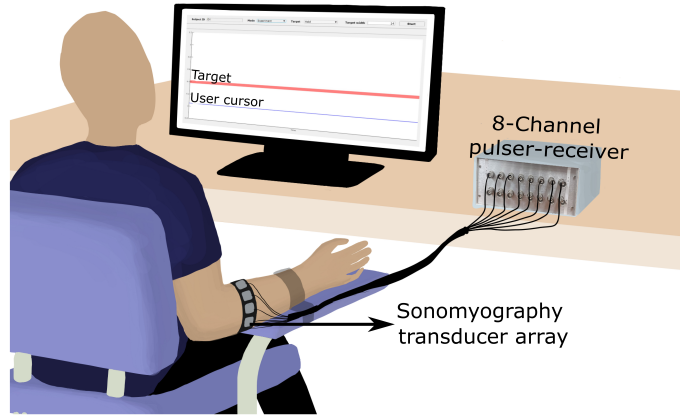


Fig. 2. Experimental setup showing the participant instrumented with the wearable sonomyography transducer array on the forearm. All the transducers were connected to the 8-channel pulser-receiver system. The sonomyography signal generated from the A-mode signals was mapped to the on-screen user cursor. The participants opened and closed their hands proportionately to reach and hold the positions of the target displayed on the computer screen

characterized using a pulse-echo setup consisting of a water-filled container in which a 2.5 cm thick acrylic reflector was immersed. The ultrasound transducers were placed on top of the setup such that the front face of the PZT was parallel to the water surface and coupled with the water using an ultrasound gel. A commercial 8-channel ultrasound pulser-receiver system (Leceour 8-channel US-MUX, Leceour Electronique, France) was used to acquire A-mode signals from the ultrasound transducers. It can acquire the A-mode signals at a sampling rate of 80 MHz. The pulser was operated in pulse-echo mode. For time and frequency domain characterization, the ultrasound transducers were excited with 90 V, 22.5 ns pulses at a pulse repetition frequency (PRF) of 1 kHz. The bandwidth of the transducers was approximately 470 ± 88 kHz ($n = 8$). The transducers were then arranged within the enclosures shown in Fig. 1 b) and were sewn to the velcro band with an inter-transducer distance of 2 cm to form the wearable sonomyography transducer array shown in Fig. 1 c).

B. Experiment setup and A-mode signal pre-processing

The subjects were seated comfortably in a chair with their hand placed on the handrest. The hand was restrained at the wrist using a cuff. The wearable sonomyography transducer array was placed around the forearm of the subjects approximately 5 cm away from the elbow in order to capture ultrasound signals from the muscle belly. All the transducers were connected to the 8-channel pulser-receiver system. The pulser was set to emit pulses with an amplitude of 90 V and pulse width of 22.5 ns. The pulse repetition frequency (PRF) was set to 15 kHz to detect the muscle activity from up to a depth of 5 cm. This resulted in a received A-mode signal length of 4000 points. The A-mode signals from all the channels were streamed into a custom-developed MATLAB (Version 2022b, Mathworks Inc., Natick MA, USA) interface. Time-

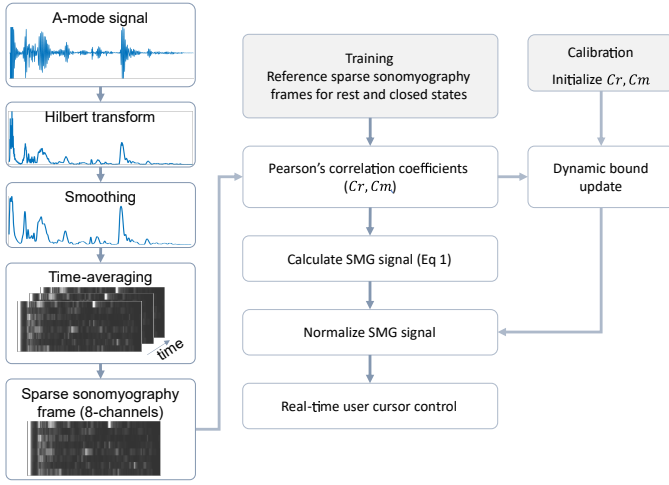


Fig. 3. Block diagram showing the steps involved in the generation of sonomyography signal

gain compensation (TGC) was provided to the received A-mode signals by setting a linearly varying gain from 25 dB to 50 dB. After TGC, the A-mode signal envelope was extracted using the Hilbert transform and the envelope was smoothed using a moving average filter having a window length of 25 samples. The pre-processed A-mode signals from all the channels were concatenated to form an 8×4000 sparse ultrasound image frame. Three consecutive sparse ultrasound frames were averaged to smooth the frames over time. The resulting time-averaged sparse ultrasound images were used to generate the sonomyography signal required to perform the online target-achievement task displayed to the subjects on a computer screen. The experiment setup is shown in Fig. 2.

C. Experimental protocol

1) *Subjects*: Five able-bodied subjects with no neuromuscular disorders participated in the study. The study protocols were approved by the Institute Ethics Committee (IEC) at the Indian Institute of Technology Delhi (IITD IEC no: P021/P050). All the subjects provided informed consent to participate in the study. The subjects were informed of the experiment protocol and performed at least one session to get familiarized with the task.

2) *Experiment*: The experiment session consisted of three stages as described below:

- **User training**: The subjects were prompted to rest for 30 s and to close their hand for 30 s via on-screen text. The pre-processed sparse ultrasound signals corresponding to the resting and closed states were stored as reference signals and were used for the rest of the session.
- **User calibration**: The sonomyography signal was generated by calculating the correlation coefficient between incoming sparse A-mode signals and the reference signals described in section II-D. The subjects were prompted to rest and close their hand thrice for a duration of 10 s and the sonomyography signal was plotted on the screen for

visualization. The final levels of the sonomyography signal corresponding to the rest and open states were saved as the lower and upper normalization bounds respectively. The range of the sonomyography signal obtained in the calibration was derated by 10% in order to minimize fatigue due to repeated maximal contractions.

- **Online target achievement task**: The user interface consists of a target and a user-controllable cursor. The targets are presented randomly at five levels from 0 to 1 in steps of 0.2 for 15 s with a 10 s rest duration after every target. The sonomyography signal was again calculated in real-time during the task and the normalized sonomyography signal was directly mapped to the position of the user cursor. The user cursor was mapped to 0 when the subject was at rest and was mapped to 1 when the subject completely closed their hand. The subjects proportionately closed their hand to reach the target levels between $[0,1]$. The subject had to reach the target levels and stay within the target as long the target remained on the screen. The thickness of the target (target width, W) was set to 5%, 10%, and 15% of the normalized range to modulate the difficulty of the tasks. To compensate for the effects of fatigue and transducer shift the normalization bounds of the sonomyography signal were dynamically updated using the dynamic bound update algorithm detailed in the section II-D.

D. Generation of sonomyography signal

The A-mode signals received from all the transducers were pre-processed and were concatenated to form an 8×4000 sparse ultrasound frame. Pearson's correlation coefficients between the incoming frame and the rest, the hand-closed reference frames acquired during user training, were calculated (see Section II-C2). The sonomyography signal is calculated as in equation 1,

$$S = \frac{(1 - C_r)}{(1 - C_r) + (1 - C_m)} \quad (1)$$

Here, C_r is the computed correlation coefficient of the incoming frame with the rest reference frame and C_m is the computed correlation coefficient of the incoming frame with the motion reference frame. The sonomyography signal, S , is normalized using the lower and upper bounds l , u obtained during user calibration. The bounds l , u were dynamically updated using the algorithm 1. The upper and lower bounds were initialized to the bounds obtained during calibration and were continuously updated for every incoming sample. The coefficient α was set to 0.01 and 0.002 for user calibration and for the online task, respectively. The choice of α was experimentally determined to eliminate the effects of drift in the baseline references.

E. Online performance metrics

The task performance of the subjects was evaluated based on the following metrics:

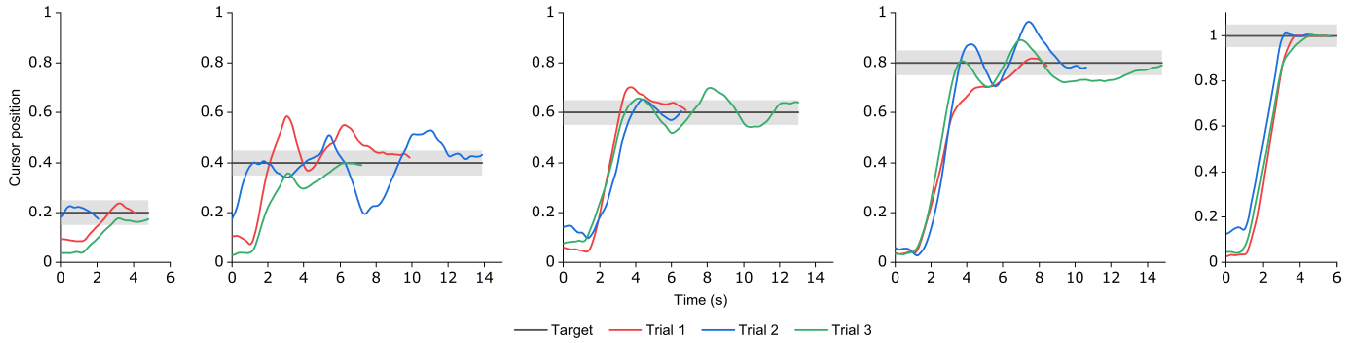


Fig. 4. Trajectories of one representative subject during all three trials of five target positions with a target width of 10%

Algorithm 1: Dynamic bound update

Input: Upper bound u , lower bound l , current sonomyography value c

Output: Upper bound u , lower bound l

```

if  $c < l$  then
  |  $l = (c + l)/2$ .
else if  $c > u$  then
  |  $u = (c + u)/2$ 
else
  | if  $|l - c| < |u - c|$  then
  | |  $l = (1 - \alpha)l + \alpha c$ 
  | else
  | |  $u = (1 - \alpha)u + \alpha c$ 
  | end
end
return  $u, l$ 

```

- **Success rate:** It is the percentage of the number of successful trials to the total number of trials. A trial was considered successful only if the subject reached the target position and stayed within the target bounds (W) for a continuous period of at least 2 seconds.
- **Movement time:** It is the time (in seconds) taken to reach the target successfully measured from the presentation of the target to the time to settle within the target bounds (W).
- **Fitt's law analysis:** The combination of the different target widths and target positions can be assigned different levels of difficulty given by the Index of difficulty (ID). Fitt's assessment provides the relationship between the index of difficulty and movement time. The index of difficulty is calculated as

$$ID = \log_2 \left(\left| \frac{D}{W} \right| + 1 \right) \quad (2)$$

Here D is the target position and W is the target width.

III. RESULTS

Fig. 4. shows all the successful trajectories achieved by one representative subject. The figure shows the three trials

of targets presented at five different positions. The trajectories demonstrate the ability of the subject to achieve the target irrespective of the target position accurately. The subjects reached the minimum and maximum targets positions in less time compared to the intermediate positions. The targets at the intermediate positions required fine control from the subjects while adapting to the responsiveness of the user cursor. Therefore, several overshoots and undershoots were seen in the trajectory.

A. Online performance assessment

The success rate with three different target widths (W) was calculated for all subjects. Fig. 5 shows the average success rate achieved by all the subjects. An average success rate of $62 \pm 18\%$ was obtained with a target width of 5% , $96 \pm 6, \%$ with target width of 10% , and $98 \pm 3\%$ with a target width of 15% . was achieved.

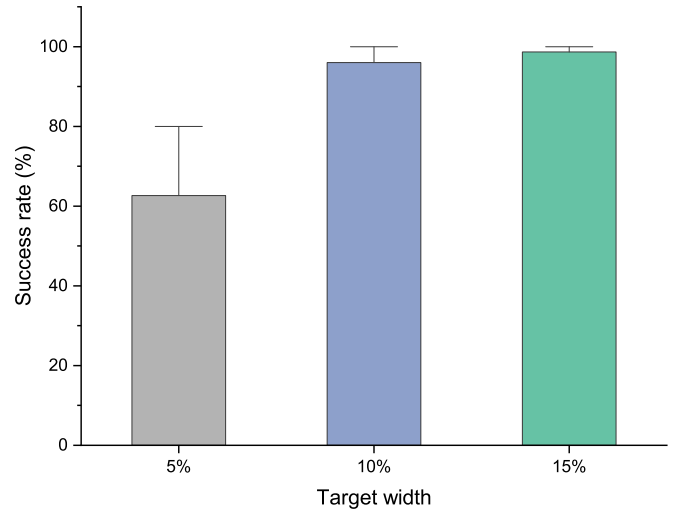


Fig. 5. Average success rate achieved by all subjects with three different target widths

The index of difficulty was calculated for all the combinations of target positions and target widths. The ID and movement time from successful trials of all subjects is plotted in Fig. 6. The mean movement time increases with increasing

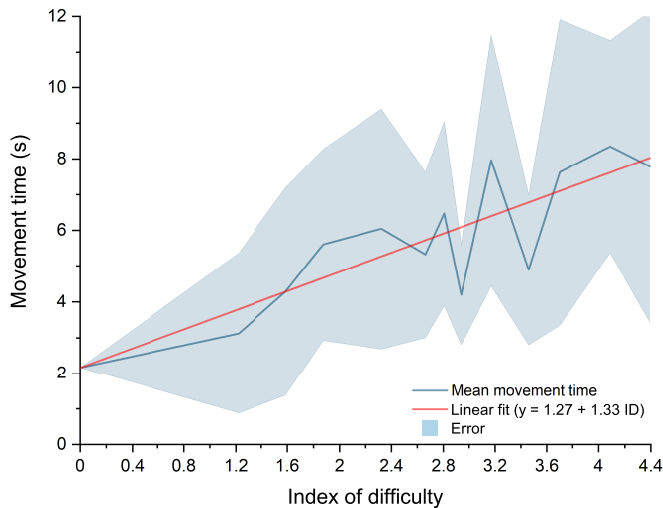


Fig. 6. Plot showing the relationship between the index of difficulty and movement time. Movement time increased as the difficulty of the task increased.

task difficulty as predicted by Fitt's law for human-computer interaction tasks [20]. A regression analysis was performed of the mean movement times versus the index of difficulty ($R^2 = 0.595$). Fitt's throughput was found to be 0.75 bits/s. The movement time intercept (y-axis intercept) was found to be 2.17 s.

IV. DISCUSSION

Real-time measurement of muscle activity using A-mode signals from the wearable, multiplexed sonomyography array has been presented. The method presented in this work uses correlation coefficients to quantify muscle activity. The resulting sonomyography signal was used to control an online human-computer target achievement task involving one degree of freedom by opening and closing the hand. The difficulty of the task was modulated by varying the target position as well as the width of the target. The index of difficulty of the targets with a width of 5% is higher and needs fine control from the subjects to stay within the allowable error bounds. Hence, the success rate for 5% target width is lower than 10%, 15% which have comparatively larger allowable error bounds. Therefore, it was noticed that the success rate in target achievement improved with an increase in target width, with success rates higher than 90% for target widths of 10% and 15%.

The responsiveness of the subjects with respect to the difficulty of the task can be seen in Fig. 6. The nearer targets with higher widths (low ID) resulted in small movement times, while targets with higher indices of difficulty resulted in higher movement times. The inherent system response time given by the y-intercept was 2.17 s, which indicates a higher reaction time compared to previously reported sonomyography systems [11]. A throughput of 0.75 bits/s was achieved, which is lower than that reported by Dhawan et al. [11]. The higher reaction time and lower throughput can be attributed to the

limited signal-to-noise ratio of A-mode signals compared to B-mode ultrasound images. To mitigate these issues, post-processing filtering may have introduced delays which resulted in increased movement times.

The proposed method has a few limitations. Though the correlation-based method is computationally inexpensive compared to model-based approaches, the computed sonomyography signal could be affected by limb movements. This method requires re-training and calibration every time the wearable system is donned. Therefore, machine-learning techniques will be employed in future work to improve the control ability and robustness of the wearable system.

V. CONCLUSION

A wearable sonomyography system with a multiplexed pulser-receiver system is presented in this work. The wearable transducer array was placed on the forearm of able-bodied individuals in order to detect muscle activity. Results show that the system is capable of fine, dexterous control of a human-computer interface.

ACKNOWLEDGMENT

A.T. Kamatham would like to acknowledge IEEE Instrumentation and Measurement Society for IEEE IMS-Graduate Fellowship Award - 2022.

REFERENCES

- [1] J. M. Hahne, M. A. Schweisfurth, M. Koppe, and D. Farina, "Simultaneous control of multiple functions of bionic hand prostheses: Performance and robustness in end users," *Science Robotics*, vol. 3, no. 19, 2018.
- [2] N. Jiang, J. L. Vest-Nielsen, S. Muceli, and D. Farina, "EMG-based simultaneous and proportional estimation of wrist/hand kinematics in uni-lateral trans-radial amputees," *Journal of NeuroEngineering and Rehabilitation*, vol. 9, no. 1, 2012.
- [3] D. Farina, N. Jiang, H. Rehbaum, A. Holobar, B. Graimann, H. Dietl, and O. C. Aszmann, "The extraction of neural information from the surface emg for the control of upper-limb prostheses: Emerging avenues and challenges," *IEEE Transactions on Neural Systems and Rehabilitation Engineering*, vol. 22, no. 4, pp. 797–809, 2014.
- [4] E. Scheme and K. Englehart, "Electromyogram pattern recognition for control of powered upper-limb prostheses: State of the art and challenges for clinical use," *Journal of Rehabilitation Research and Development*, vol. 48, pp. 643–660, 2011.
- [5] L. Resnik, H. H. Huang, A. Winslow, D. L. Crouch, F. Zhang, and N. Wolk, "Evaluation of EMG pattern recognition for upper limb prosthesis control: A case study in comparison with direct myoelectric control," *Journal of NeuroEngineering and Rehabilitation*, vol. 15, no. 1, pp. 1–13, 2018.
- [6] L. A. Hallock, A. Velu, A. Schwartz, and R. Bajcsy, "Muscle deformation correlates with output force during isometric contraction," in *2020 8th IEEE RAS/EMBS International Conference for Biomedical Robotics and Biomechanics (BioRob)*, 2020, pp. 1188–1195.
- [7] Q. Chang, J. Shi, Z. Xiao, and Y. Zheng, "A research of smg controlled prosthetic hand with sse2 acceleration," in *2008 9th International Conference on Signal Processing*, 2008, pp. 2146–2149.
- [8] N. Akhlaghi, C. A. Baker, M. Lahlou, H. Zafar, K. G. Murthy, H. S. Rangwala, J. Kosecka, W. M. Joiner, J. J. Pancrazio, and S. Sikdar, "Real-time classification of hand motions using ultrasound imaging of forearm muscles," *IEEE Transactions on Biomedical Engineering*, vol. 63, no. 8, pp. 1687–1698, 2016.
- [9] C. Castellini and D. S. Gonzalez, "Ultrasound imaging as a human-machine interface in a realistic scenario," in *2013 IEEE/RSJ International Conference on Intelligent Robots and Systems*, 2013, pp. 1486–1492.

- [10] C. Castellini and G. Passig, "Ultrasound image features of the wrist are linearly related to finger positions," in *2011 IEEE/RSJ International Conference on Intelligent Robots and Systems*, 2011, pp. 2108–2114.
- [11] A. S. Dhawan, B. Mukherjee, S. Patwardhan, N. Akhlaghi, G. Diao, G. Levay, R. Holley, W. M. Joiner, M. Harris-Love, and S. Sikdar, "Proprioceptive Sonomyographic Control: A novel method for intuitive and proportional control of multiple degrees-of-freedom for individuals with upper extremity limb loss," *Scientific Reports*, vol. 9, no. 1, p. 9499, 2019.
- [12] S. M. Engdahl, S. A. Acuña, E. L. King, A. Bashatah, and S. Sikdar, "First Demonstration of Functional Task Performance Using a Sonomyographic Prosthesis: A Case Study," *Frontiers in Bioengineering and Biotechnology*, vol. 10, no. May, pp. 1–20, 2022.
- [13] N. Akhlaghi, A. Dhawan, A. A. Khan, B. Mukherjee, G. Diao, C. Truong, and S. Sikdar, "Sparsity analysis of a sonomyographic muscle-computer interface," *IEEE Transactions on Biomedical Engineering*, vol. 67, no. 3, pp. 688–696, 2020.
- [14] A. T. Kamatham, M. Alzamani, A. Dockum, S. Sikdar, and B. Mukherjee, "Sparse sonomyography-based estimation of isometric force: A comparison of methods and features," *IEEE Transactions on Medical Robotics and Bionics*, vol. 4, no. 3, pp. 821–829, 2022.
- [15] J. Yan, X. Yang, X. Sun, Z. Chen, and H. Liu, "A lightweight ultrasound probe for wearable human-machine interfaces," *IEEE Sensors Journal*, vol. 19, no. 14, pp. 5895–5903, 2019.
- [16] I. AlMohimeed, H. Turkistani, and Y. Ono, "Development of wearable and flexible ultrasonic sensor for skeletal muscle monitoring," in *2013 IEEE International Ultrasonics Symposium (IUS)*, 2013, pp. 1137–1140.
- [17] X. Yang, Z. Chen, N. Hettiarachchi, J. Yan, and H. Liu, "A wearable ultrasound system for sensing muscular morphological deformations," *IEEE Transactions on Systems, Man, and Cybernetics: Systems*, vol. 51, no. 6, pp. 3370–3379, 2021.
- [18] X. Yang, Y. Zhou, and H. Liu, "Wearable ultrasound-based decoding of simultaneous wrist/hand kinematics," *IEEE Transactions on Industrial Electronics*, vol. 68, no. 9, pp. 8667–8675, 2021.
- [19] X. Yang, J. Yan, Z. Yin, and H. Liu, "Sonomyographic prosthetic interaction: Online simultaneous and proportional control of wrist and hand motions using semisupervised learning," *IEEE/ASME Transactions on Mechatronics*, pp. 1–10, 2022.
- [20] P. M. Fitts, "The information capacity of the human motor system in controlling the amplitude of movement. 1954." *Journal of experimental psychology. General*, vol. 121 3, pp. 262–9, 1992.